microbial biotechnology

Exogenous maltose enhances Zebrafish immunity to levofloxacin-resistant *Vibrio alginolyticus*

Ming Jiang,[1,2,†] Lifen Yang,[1,†]
Zhuang-gui Chen,[1] Shi-shi Lai,[1] Jun Zheng[3] and
Bo Peng[1,2,4]*

[1]*The Third Affiliated Hospital, State Key Laboratory of Biocontrol, Guangdong Key Laboratory of Pharmaceutical Functional Genes, School of Life Sciences, Sun Yat-sen University, Guangzhou, 510275, China.*
[2]*Laboratory for Marine Biology and Biotechnology, Qingdao National Laboratory for Marine Science and Technology, Qingdao, 266071, China.*
[3]*Faculty of Health Sciences, University of Macau, Macau SAR, China.*
[4]*Southern Marine Science and Engineering Guangdong Laboratory (Zhuhai), Zhuhai, 519000, China.*

Summary

Understanding the interplay between bacterial fitness, antibiotic resistance, host immunity and host metabolism could guide treatment and improve immunity against antibiotic-resistant pathogens. The acquisition of levofloxacin (Lev) resistance affects the fitness of *Vibrio alginolyticus in vitro* and *in vivo*. Lev-resistant (Lev-R) *V. alginolyticus* exhibits slow growth, reduced pathogenicity and greater resistance to killing by the host, *Danio rerio* (zebrafish), than Lev-sensitive (Lev-S) *V. alginolyticus*, suggesting that Lev-R *V. alginolyticus* triggers a weaker innate immune response in *D. rerio* than Lev-S *V. alginolyticus*. Differences were detected in the metabolome of *D. rerio* infected with Lev-S or Lev-R *V. alginolyticus*. Maltose, a crucial metabolite, is significantly downregulated in *D. rerio* infected with Lev-R *V. alginolyticus,* and exogenous maltose enhances the immune response of *D. rerio* to Lev-R *V. alginolyticus*, leading to better clearance of the infection. Furthermore, we demonstrate that exogenous maltose stimulates the host production of lysozyme and its binding to Lev-R *V. alginolyticus*, which depends on bacterial membrane potential. We suggest that exogenous exposure to crucial metabolites could be an effective strategy for treating and/or managing infections with antibiotic-resistant bacteria.

Introduction

The overuse or misuse of antibiotics in clinical and agricultural settings has promoted the emergence and spread of antibiotic-resistant bacteria, some of which are disease-causing bacterial pathogens (Kraemer *et al.*, 2019). Meanwhile, resistance to most of the currently used antibiotics now threatens food safety (Wyrsch *et al.*, 2016). Because diverse mechanisms underlie the antibiotic resistance of different bacterial strains and organisms, it has been challenging to develop novel efficient antibiotics (Lee and Collins, 2011). Under such circumstances, alternative approaches to treat and control infections caused by antibiotic-resistant pathogens are urgently needed.

The innate immune system, which is conserved throughout evolution, plays a role in activating and initiating the adaptive immune response to bacterial infection (Thomas and Yang, 2016). Because the adaptive immune system is absent in invertebrate species, the role of innate immunity, and its potential use in fighting bacterial infections, can be readily investigated in invertebrates, such as *Danio rerio,* commonly known as zebrafish (ZF) (Kovarik *et al.*, 2016; Gammoh and Rink, 2017). Mechanisms of bacterial antibiotic resistance often involve significant genetic changes and may carry a fitness cost, leading to virulence or persistence (Andersson, 2003; Gandon and Vale, 2014), slow growth, compromised pathogenicity and poor transmission (Andersson and Hughes, 2010; Roux *et al.*, 2015). Antibiotic-resistant bacterial pathogens also frequently evolve rapidly, adapting to the host environment and avoiding detection and/or destruction by host immune systems. We suggest that the genetic and phenotypic changes that confer antibiotic resistance trigger different host immune responses, and a better understanding of these processes could facilitate efforts to develop effective strategies to manage infections caused by antibiotic-resistant bacteria.

Metabolism plays an essential role in shaping the innate immune response and strengthening host defence mechanisms (Cheng *et al.*, 2014; Cameron *et al.*, 2016; Zhang *et al.*, 2017; Araldi *et al.*, 2017). For example, in macrophages, lanosterol decreases expression and activation of signal transducer and activator of transcription 1 (STAT1) and STAT2 by IFN β, which increases survival by reducing cytokine secretion (Araldi *et al.*, 2017). Besides, under hypoxic conditions, the innate immune response to bacterial infection can be enhanced through the activation of HIF-1α and neutrophil metabolism (Araldi *et al.*, 2017). Carbohydrates are also important for modulating immunity (Crocker and Feizi, 1996). For example, protein-linked oligosaccharides associated with microbes can be recognized by T-lymphocytes, contributing to immune surveillance (Avci *et al.*, 2013). Metabolite like L-aspartic acid promotes the production of nitrogen oxide and enhances phagocytosis to clear bacterial infection (Gong *et al.*, 2020). But whether metabolism plays roles in distinguishing antibiotic-sensitive and antibiotic-resistant bacteria is not yet explored.

Here, we propose that metabolic modulation could be considered as a strategy to boost the effectiveness of the innate immune system (Peng *et al.*, 2015; Su *et al.*, 2015). We hypothesize that different host metabolic responses to antibiotic-sensitive and antibiotic-resistant bacteria could be exploited to enhance the clearance of bacterial pathogens. In this study, we test this hypothesis using levofloxacin-resistant (Lev-R) and levofloxacin-sensitive (Lev-S) *Vibrio alginolyticus* and a zebrafish (ZF) model system. *V. alginolyticus* causes high morbidity in marine fish, and otitis and wound infection in humans (Newton *et al.*, 2012; Wang *et al.*, 2016). Antibiotic-resistant *V. alginolyticus* arises frequently (Sperling *et al.*, 2015), representing a threat to human health and the safe production of farmed fish. Our findings may pave the way for the development of novel alternative strategies for managing antibiotic-resistant bacterial infections.

Results

Levofloxacin-resistant *Vibrio alginolyticus* display reduced pathogenicity and immunogenicity

In an experimental evolution approach, we generated *V. alginolyticus* levofloxacin-resistant (Lev-R), which was 16MIC of the levofloxacin-sensitive (Lev-S) bacterial strain (see Experimental procedures) (Fig. 1A; Fig. S1). Whole-genome sequencing of Lev-R *V. alginolyticus* (Table S1) identified eight mutations, five of which occurred in the following gene coding regions: *AT730_01475*, *aceF*, *cpxP*, *cpxA* and *gyrB*. Of these, *gyrB* is the only gene previously associated with fluoroquinolone resistance (Tables S1 and S2). While *cpxP* harbours a frameshift mutation, the other

four genes harbour point mutations. CpxA and CpxP are bacterial envelope stress proteins previously associated with antibiotic resistance (Danese and Silhavy, 1998; Raivio *et al.*, 2013; Zhang *et al.*, 2019). The functions of *AT730_01475* and *aceF* in antibiotic resistance have not yet been elucidated.

Fitness of Lev-R *V. alginolyticus* was investigated by injecting 9×10^5 CFU Lev-R or Lev-S *V. alginolyticus* into ZF (Fig. S2). At this dose, infection with Lev-S *V. alginolyticus* caused 90% mortality and 10% survival after 2 days, whereas ZF infected with Lev-R *V. alginolyticus* had 92% survival 6 days' post-injection (Fig. 1B), indicating attenuated pathogenicity of Lev-R *V. alginolyticus*. To investigate the adaptation of Lev-R during infection of ZF, bacterial *gyrB* gene copies, which were not affected by the presence of point mutations (Fig. S3A), were quantified at different time points after infection. qPCR data indicated 2×10^5 copies of bacterial *gyrB* immediately after injection (0 h) of ZF with Lev-S or Lev-R *V. alginolyticus*. The rapid proliferation of bacteria was observed from 6 to 24 h post-injection, with more Lev-S- than Lev-R *V. alginolyticus* detected in ZF 24 h post-injection. However, the number of Lev-S *V. alginolyticus* decreased to trace amounts by 48 h and was undetectable at 72 h post-infection, while the number of Lev-R *V. alginolyticus* was similar at 0 and 48 h post-injection, and was still detectable 72 h post-injection (Fig. 1C). The bacterial load of injected ZF was also estimated by measuring colony-forming units (CFUs) in extracts of infected ZF at 0, 6, 24, 48 or 72 h post-injection. A similar pattern of bacterial growth post-injection was documented using qPCR- or CFU-based methods to count bacteria (Fig. S4A). Interestingly, bacteria were detected in the liver but not muscle, intestine, spleen or head kidney of infected ZF 72 h post-infection (Fig. S4B).

To investigate the mechanism that allows Lev-S *V. alginolyticus* to be cleared from infected ZF more quickly than Lev-R *V. alginolyticus*, spleen (Fig. 1D) and head kidney (Fig. 1E), which are major immunological organs of ZF, were isolated from infected or control ZF, and expression of innate immune genes was analysed by qRT-PCR, as previously described (Faikoh *et al.*, 2014). Specifically, expression of 12 genes, *Il1b*, *Il6*, *il8*, *il10*, *il21*, *tnfa*, *Ptgr2*, *ifng*, lysozyme, *hamp1*, *hamp2* and *leap2*, including four antimicrobial peptides, was analysed at 6 h post-injection. In spleen, Lev-S and Lev-R *V. alginolyticus* induced a stronger immune response than the control, and Lev-S *V. alginolyticus* induced a stronger immune response than Lev-R *V. alginolyticus* (Fig. 1D). Similar results were obtained in head kidney, except that expression of *hamp1* and *hamp2* was unaffected (Fig. 1E). However, in head kidney and spleen, no bacteria were detected by qRT-PCR or plating at this time point (data not shown). Moreover, similar gene expression data were obtained following Lev-S or Lev-R
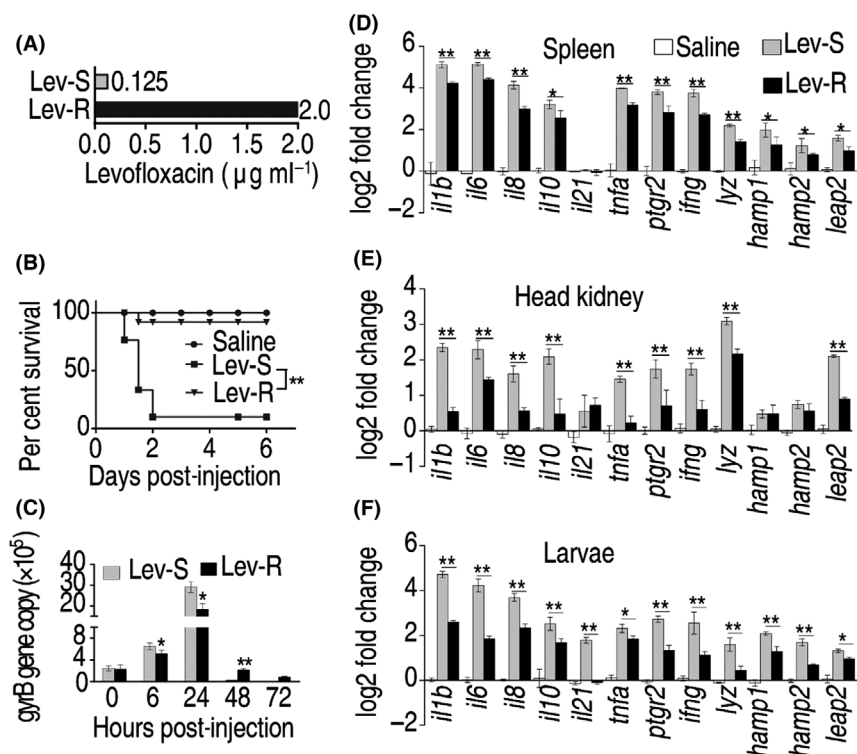
Fig. 1. Zebrafish response to Lev-R.

A. The MIC of levofloxacin-sensitive *V. alginolyticus* (Lev-S) and levofloxacin-resistant bacteria (Lev-R). 0.125 µg levofloxacin, which is equal to the MIC of Lev-S, is defined as 1 MIC.

B. Per cent survival of ZF infected with 9×10^5 CFU of Lev-R or Lev-S or saline control. Statistical analysis was performed with the log-rank test, $*P < 0.05$; $**P < 0.01$.

C. qPCR for clearance of Lev-R in ZF compared with that of Lev-S. 2×10^5 CFU of Lev-R or Lev-S was used to infect ZF. The total DNA was extracted for qPCR at the indicated time points (0, 6, 24, 48 and 72 h). The main effect of bacterial type and time was significant ($P < 0.01$), and the interaction effects for bacterial type and time were significant ($P < 0.01$).

D. qRT-PCR for innate immune genes of spleen infected by Lev-R or Lev-S. 2×10^5 CFU of Lev-R or Lev-S was used to infect zebrafish, and then, mRNA of spleen was extracted for qRT-PCR at 6 h post-infection. The main effect of bacterial type and immune gene expression was significant ($P < 0.01$), and the interaction effects for bacterial type and host immune gene expression were significant ($P < 0.01$).

E. qRT-PCR for innate immune genes of head kidney infected by Lev-R or Lev-S. 2×10^5 CFU of Lev-R or Lev-S was used to infect zebrafish, and then, mRNA of head kidney was extracted for qRT-PCR at 6 h post-infection. The main effect of bacterial type and immune gene expression was significant ($P < 0.01$), and the interaction effects for bacterial type and host immune gene expression were significant ($P < 0.01$).

F. qRT-PCR for innate immune genes of newborn ZF larvae infected by Lev-R or Lev-S. 1×10^5 CFU of Lev-R or Lev-S was used to infect zebrafish, and then, mRNA was extracted for qRT-PCR at 6 h post-infection. The main effect of bacterial type and immune gene expression was significant ($P < 0.01$), and the interaction effects for bacterial type and host immune gene expression were significant ($P < 0.01$). All of the above statistical analysis was analysed by ART-ANOVA or Kruskal–Wallis followed by Dunn's multiple comparison *post hoc* test unless otherwise indicated. $*P < 0.05$; $**P < 0.01$. Error bars represent means $\pm$ SEM from at least three biological replicates.

V. alginolyticus infection of newborn ZF larvae, whose adaptive immunity is absent so that Lev-S and Lev-R induce differential innate immune response can be confirmed (Fig. 1F). Thus, ZF demonstrates slower clearance as well as a weaker immune response to Lev-R *V. alginolyticus*; this suggests improved fitness of Lev-R *V. alginolyticus* during infection of ZF.

Different metabolomes in ZF infected by Lev-R and Lev-S *V. alginolyticus*

GC-MS was used to investigate and compare Lev-R- and Lev-S *V. alginolyticus*-induced changes in the ZF metabolome, to identify crucial metabolites as potential

biomarkers and to understand the slower clearance of Lev-R *V. alginolyticus* from infected ZF. For this purpose, ZF was injected with an LD$_{50}$ dose of Lev-S or Lev-R *V. alginolyticus* or saline (as a control), and the metabolomes of surviving ZF were analysed by GC-MS. Ten biological replicates and two technical replicas of each group were performed, yielding 60 data sets. Metabolites that were differentially affected by bacterial infection were identified (Fig. S8). Compared with the control group, 61 or 67 metabolites demonstrated differential abundance in ZF infected with Lev-S or Lev-R *V. alginolyticus* respectively. A Z-score plot based on the control showed values from −4.60 to 18.26 for metabolites in Lev-S *V. alginolyticus*-infected ZF and from

−2.03 to 56.05 for metabolites in Lev-R *V. alginolyticus*-infected ZF (Fig. 2A). Among the differential abundance of metabolites, 54 metabolites were overlapped, in which 17 were decreased and 23 were increased. In addition, the abundance of 14 metabolites was reversal between Lev-S and Lev-R, and the others were Lev-S- and Lev-R-specific, including four increased and three decreased in Lev-S, and eight increased and five decreased in Lev-R (Fig. 2B). Principal component analysis (PCA) detected obvious separation between the Lev-S *V. alginolyticus*-induced metabolome and Lev-R *V. alginolyticus*-induced metabolome (Fig. 2C), with no significant outliers. Component t[1] separated Lev-R *V. alginolyticus*-infected ZF from the control group, while component t[2] separated Lev-S *V. alginolyticus*-infected ZF from the other two groups. Discriminating variables were present in the S-plot using a cut-off value of ≥ 0.05 for the absolute value of covariance p and a cut-off value of ≥ 0.5 for p(corr) (Fig. 2D). Crucial metabolite biomarkers were screened by component p[1] and component p[2]. In component p[1], glucose, maltose, pyroglutamic acid, valine, alanine, tyrosine, threonine, serine, cholesterol, inosine, lactic acid, histidine, hypoxanthine, taurine, phosphoric acid were identified and in component p[2], maltose, histidine, glycerol 3-phosphate, GABA, stearic acid, mannose 6-phosphate, fructose 6-phosphate, glycine, taurine were identified. Maltose was selected as the most significant biomarker because its abundance
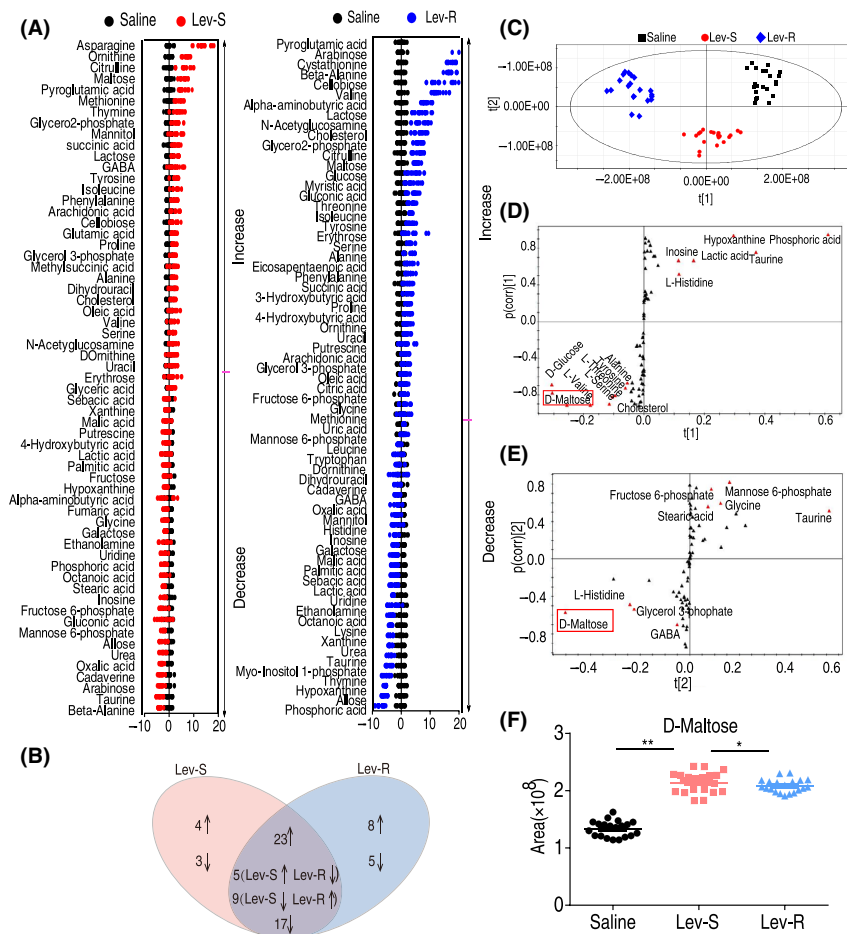

Fig. 2. Differential metabolomes of zebrafish infected by Lev-R.
A. *Z* scores (standard deviation from average). Each point represents one technical repeat in one metabolite. Black, Control; blue, Lev-R; Red, Lev-S.
B. Venn diagram of differential metabolites of Lev-S and Lev-R. Decreased and increased metabolites are indicated with down and up arrows respectively.
C. Principle component analysis (PCA) of Lev-R, Lev-S and saline control. Each dot represents one technical replicate.
D and E. The distribution of the differential abundance of metabolites' weight from the method of OPLS-DA to control and experimental samples. Triangle represents metabolites and candidate biomarkers are highlighted with red.
F. Abundance of maltose in Lev-R, Lev-S and saline control. Statistical analysis was performed with Student's *t*-test, *$P < 0.05$; **$P < 0.01$.
Error bars represent means $\pm$ SEM from at least three biological replicates.

was elevated in both component p[1] and component p [2] (Fig. 2D,E), being consistent with our criteria that elevated biomarkers not only distinguished Lev-R-induced metabolome from Lev-S-induced metabolome, but also separated infectious metabolome, including Lev-R-metabolome and Lev-S-metabolome, from non-infected metabolome, the saline control. Indeed, maltose was more abundant in the metabolomes of Lev-R and Lev-S *V. alginolyticus*-infected ZF than in control, and also more abundant in Lev-S *V. alginolyticus*-infected ZF than in Lev-R *V. alginolyticus*-infected ZF (Fig. 2F). These results suggest different metabolomic strategies in response to infection by Lev-S and Lev-R *V. alginolyticus*, and that maltose is the most crucial metabolite biomarker.

Increased availability of maltose in Lev-S V. alginolyticus-infected ZF

To explore mechanisms underlying differential abundance of maltose, we measured the transcription of alpha-amylase, which breaks down starch to form maltose and glucose, as well as maltase-glucoamylase and alpha-glucosidase, which metabolize maltose (Fig. 3A). Interestingly, the expression of alpha-amylase (*amy2*a) was upregulated in Lev-S *V. alginolyticus*-infected ZF but not in Lev-R *V. alginolyticus*-infected ZF, and the expression of maltase-glucoamylase (encoded by *gaa* and *ganc*) and alpha-glucosidase (encoded by *si*) was downregulated to a similar extent in Lev-S- and Lev-R *V. alginolyticus*-infected ZF (Fig. 3B). More importantly, the promoter of *amy2A* was induced strongly by Lev-S- but not by Lev-R *V. alginolyticus* at 3 h post-infection (Fig. 3C), after which

cell viability decreased and the Lev-S and Lev-R induced differential luciferase activity (Fig. S5). Taken together, these results demonstrate that Lev-S *V. alginolyticus*-infected ZF induces higher maltose production through upregulating *amy2a* transcription to a greater extent than Lev-R *V. alginolyticus*. This could imply that the increased abundance of maltose is a metabolic response of the host to *V. alginolyticus* infection.

Exogenous maltose potentiates the ability of ZF to kill Lev-R V. alginolyticus

Crucial biomarkers can programme the metabolome as a strategy to manage internal or external stressors (Thompson *et al.*, 2017), which motivated us to examine whether exogenous maltose could potentiate the ability of ZF to kill Lev-R *V. alginolyticus*. To examine this possibility, ZF was injected with exogenous maltose. LC-MS showed that injection of ZF with maltose increased the *in vivo* maltose level approximately twofold (Fig. 4A) and increased the rate at which bacterial load of Lev-R *V. alginolyticus* decreased, being similar to that of Lev-S *V. alginolyticus* at 48 and 72 h (Fig. 4B). Similar results were obtained when the bacterial load was quantified using CFUs (Fig. S6). These results indicate that exogenous maltose potentiates the elimination of Lev-R *V. alginolyticus* from infected ZF.

Exogenous maltose regulates zebrafish innate immune gene expression

We reasoned that the metabolomic change in infected ZF might be tightly associated with the innate immune
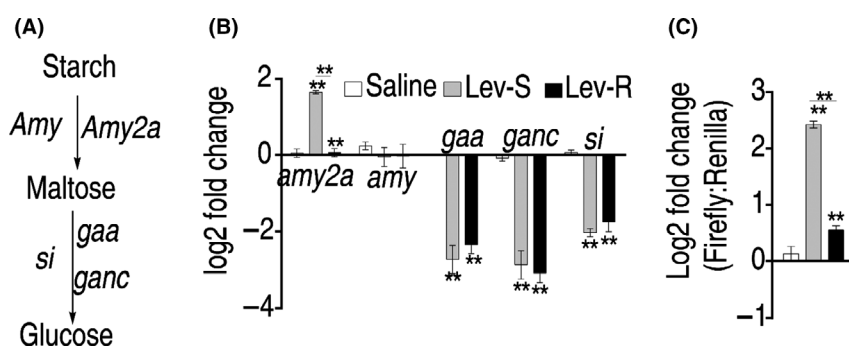

Fig. 3. *V. alginolyticus* enhances maltose production.
A. Schematic representation of maltose metabolism.
B. qRT-PCR of the genes that break down starch to form maltose, and genes that metabolizing maltose. ZF was challenged with either 2×10^5 CFU of Lev-S or Lev-R. After 6 h, the RNA was extracted for qRT-PCR. Statistic analysis was analysed by ART-ANOVA and Kruskal–Wallis followed by Dunn's multiple comparison *post hoc* test. The main effect of bacterial type and immune genes expression were significant ($P < 0.01$), and the interaction effects for bacterial type and host immune genes expression were significant ($P < 0.01$). *$P < 0.05$; **$P < 0.01$.
C. Promoter activity assay of *amy2a* gene. The upstream 1.5 kb sequence of the transcription starting site of *amy2a* gene was cloned into pGL promoterless vector. The construct was transfected into the zebrafish ZF4 cell line. After 48 h post-transfection, transfected cells were infected with either Lev-S or Lev-R. Six hours later, the cells were collected for luminescent measurement. The ratio of firefly to renilla was plotted. Statistical analysis was performed by Kruskal–Wallis followed by Dunn's multiple comparison *post hoc* test. *$P < 0.05$; **$P < 0.01$. Error bars represent means ± SEM from at least three biological replicates.
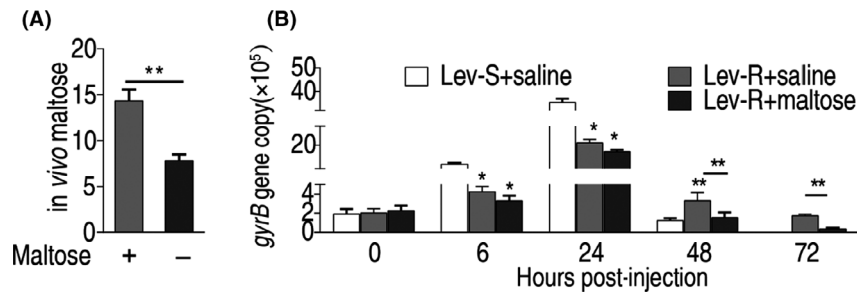
Fig. 4. Per cent survival of zebrafish and clearance of Lev-R in the presence of exogenous maltose
A. Maltose level of zebrafish injected with and without exogenous maltose. Statistic analysis was analysed by Kruskal–Wallis followed by Dunn's multiple comparison *post hoc* test, **$P < 0.01$. Error bars represent means $\pm$ SEM from at least three biological replicates.
B. Clearance of Lev-R in the presence or absence of maltose compared with that of Lev-S in the absence of maltose. Zebrafish were injected with 2×10^5 CFU of Lev-R. DNA was extracted for qPCR at 0, 6, 24, 48 and 72 h. Statistic analysis was analysed by ART-ANOVA and Kruskal–Wallis followed by Dunn's multiple comparison *post hoc* test. The main effect of bacterial type and time was significant ($P < 0.01$), and the interaction effects for bacterial type and time were significant ($P < 0.01$). *$P < 0.05$; **$P < 0.01$. Error bars represent means $\pm$ SEM from at least three biological replicates.

response to bacterial infection. First, the possibility that maltose affects bacterial growth was examined (Fig. S7A,B), showing that Lev-R *V. alginolyticus* grows more slowly than Lev-S *V. alginolyticus*, independent of the presence or absence of exogenous maltose. Second, the expression of six *V. alginolyticus* virulence genes (*ctxA, trh, tlh, vpi, toxR* and *tdh*) (Xie *et al.*, 2005; Abdallah *et al.*, 2009) was also similar in rich and minimal medium (Fig. S7C,D). However, when transcription of innate immunity genes was quantified in ZF spleen in the presence or absence of exogenous maltose, the results showed >twofold higher expression of *lysozyme* and the antimicrobial peptides (*hamp1* and *hamp2*) in maltose-treated ZF than in saline-treated ZF, no change in expression of *il1b, il8, il10* and *tnfa*, and lower expression of *il6, il21, Ptgr2* and *ifng* (Fig. 5A). In the ZF head kidney, injection of maltose also significantly increased the expression of *lysozyme* (Fig. 5B).

Lysozyme promotes the killing of Lev-R V. alginolyticus

Previous reports indicate that lysozyme promotes the killing of *V. alginolyticus* (Sava, 1996; Krens *et al.*, 2017), prompting us to focus on lysozyme in the following studies. Our evidence shows that maltose increases the activity of lysozyme (Fig. 6A) and that Lev-S *V. alginolyticus* is sensitive to killing by lysozyme at 6.25–400 μg ml^{-1}, while Lev-R *V. alginolyticus* is less sensitive to killing by lysozyme (e.g. ≥ 100 μg ml^{-1} lysozyme) (Fig. 6B). Thus, Lev-R has increased resistance towards dose-dependent killing by lysozyme.

Mechanisms for the clearance of lysozyme to Lev-R

Lysozyme degrades components of the bacterial cell wall, which promotes clearance of bacteria from the infected
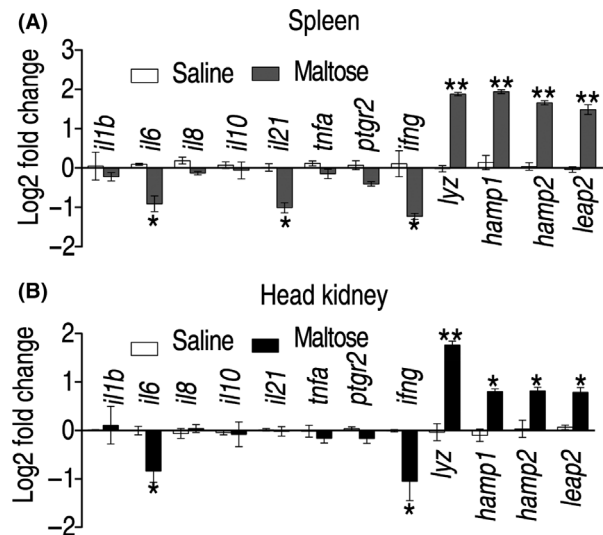

Fig. 5. Exogenous maltose promotes zebrafish innate immune response against Lev-R infection.
A. qRT-PCR for innate immune genes in the spleen of zebrafish in the presence or absence of maltose. The main effect of bacterial type and immune gene expression was significant ($P < 0.01$), and the interaction effects for bacterial type and host immune gene expression were significant ($P < 0.05$).
B. qRT-PCR for innate immune genes in head kidneys of zebrafish in the presence or absence of maltose. The main effect of bacterial type and immune gene expression was significant ($P < 0.01$), and the interaction effects for bacterial type and host immune gene expression were significant ($P < 0.05$). All of the statistical analysis was analysed by ART-ANOVA or Kruskal–Wallis followed by Dunn's multiple comparison *post hoc* test. *$P < 0.05$; **$P < 0.01$. Error bars represent means $\pm$ SEM from at least three biological replicates.

host. The binding of lysozyme to the bacterial cell wall involves electrostatic interactions that might be influenced by bacterial membrane potential (Bergers *et al.*, 1993; Gorbenko *et al.*, 2007). As the membrane potential is higher for antibiotic-sensitive bacteria than for antibiotic-resistant
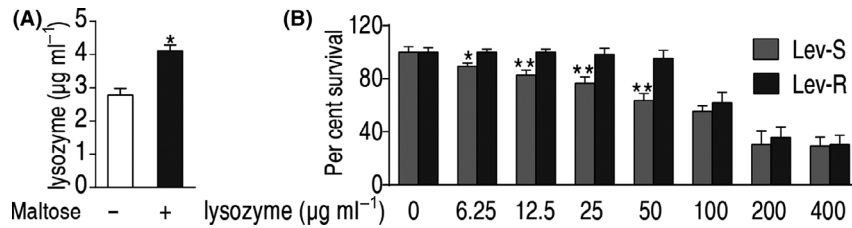
Fig. 6. Lysozyme plays critical roles in killing Lev-R.
A. Quantitative analysis of lysozyme of zebrafish infected with Lev-R in the presence or absence of maltose.
B. Bactericidal ability of lysozyme to Lev-R and Lev-S in the presence of different concentrations of lysozyme. All of the statistical analysis was analysed by Kruskal–Wallis followed by Dunn's multiple comparison *post hoc* test. *$P < 0.05$; **$P < 0.01$. Error bars represent means $\pm$ SEM from at least three biological replicates.

bacteria (Peng *et al.*, 2015), we hypothesize different binding affinities of lysozyme to Lev-S and Lev-R *V. alginolyticus*. To test this idea, the dose-dependent binding of lysozyme to Lev-S and Lev-R *V. alginolyticus* was examined at 4°C. The results show relatively lower binding to Lev-R than to Lev-S *V. alginolyticus* at <50 μg ml^{-1} lysozyme (Fig. 7A). Furthermore, Lev-R *V. alginolyticus* demonstrated lower membrane polarization than Lev-S *V. alginolyticus* (Fig. 7B), while treatment with 0.125 to 2.0 mM carbonyl cyanide 3-chlorophenylhydrazone
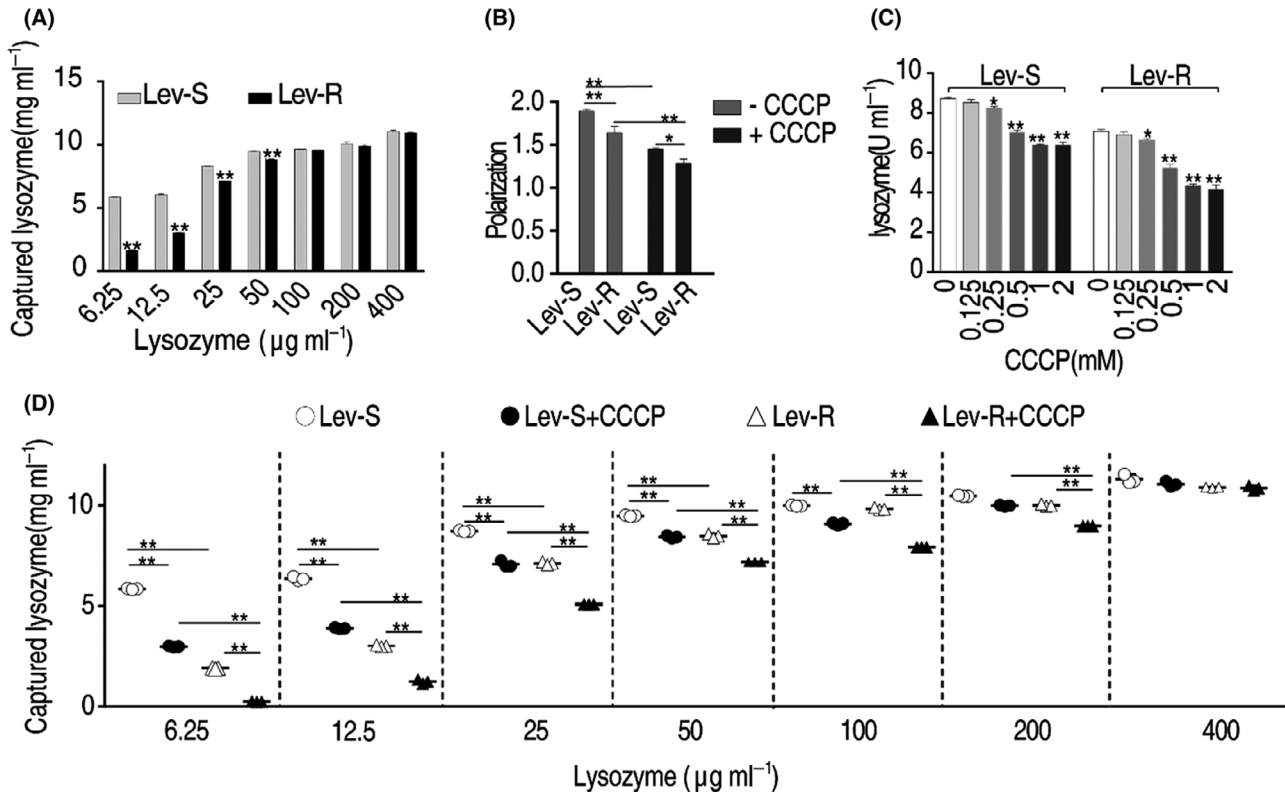

Fig. 7. Mechanisms for the clearance of lysozyme to Lev-R.
A. Quantitative analysis of lysozyme captured by Lev-S and Lev-R.
B. Membrane polarization of Lev-S and Lev-R in the presence or absence of CCCP.
C. Quantitative analysis of lysozyme captured by Lev-S and Lev-R in the presence of different concentrations of CCCP. The main effect of bacteria type and concentration of CCCP were significant ($P < 0.01$), and the interaction effects for bacteria type and concentration of CCCP were significant ($P < 0.05$).
D. Effect of lysozyme concentration on the binding of Lev-S and Lev-R to lysozyme in the presence of CCCP. The main effect of bacteria type and concentration of lysozyme were significant ($P < 0.01$), and the interaction effects for bacteria type and concentration of lysozyme were significant ($P < 0.01$). All of the above analysis was analysed by ART-ANOVA or Kruskal–Wallis followed by Dunn's multiple comparison *post hoc* test. *$P < 0.05$; **$P < 0.01$. Error bars represent means $\pm$ SEM from at least three biological replicates.

(CCCP) decreased membrane polarization and reduced binding of lysozyme to both strains in a dose-dependent manner (Fig. 7B,C). Comparatively, lower binding was detected in Lev-R than in the Lev-S with lysozyme activity from 7.0 to 4.1 μg ml^{-1} (reduced 2.9 μg ml^{-1}), and from 8.7 μg ml^{-1} to 6.3 μg ml^{-1} (reduced 2.4 μg ml^{-1}) respectively (Fig. 7C). These data confirm that lower membrane polarization lowers the binding affinity between bacterial membrane and lysozyme and show that binding affinity also depends on the concentration of lysozyme (Fig. 7D). These results indicate that the lower rate of clearance of Lev-R *V. alginolyticus* from ZF can be attributed to lower membrane polarization leading to lower binding of lysozyme to Lev-R *V. alginolyticus*.

Discussion

The present study hypothesizes that the host mounts different innate immune responses to antibiotic-sensitive and antibiotic-resistant pathogens, and these responses are associated with different metabolomes. The metabolome can be reprogrammed by exposure to exogenous metabolites, promoting the elimination of antibiotic-resistant bacteria, which represents a major step in understanding bacterial fitness and its interplay with the innate immune response. Our results show that Lev-R *V. alginolyticus* grows slower than Lev-S (Fig. S7A,B) *in vitro* and greater survival *in vivo* in ZF, suggesting associated fitness cost. The fitness cost associated with antibiotic resistance affected the metabolomic strategy of infected ZF and its innate immune response, so that survival of antibiotic-resistant *V. alginolyticus* in ZF was greater than the survival of antibiotic-sensitive *V. alginolyticus*. There was a close link between the metabolome and the innate immune response, which was demonstrated by discovery metabolomics and the effect of metabolomic reprogramming by exogenous maltose (Peng *et al.*, 2015). These findings indicate that antibiotic-resistant *V. alginolyticus* triggers a weaker innate immune response in ZF than antibiotic-sensitive *V. alginolyticus*, which is reflected by their different metabolomes. Thus, metabolomic reprogramming is an effective measure to promote the elimination of antibiotic-resistant pathogens.

The innate immune system provides immediate defence against bacterial infection (Cameron *et al.*, 2016); however, infection with Lev-R *V. alginolyticus* provoked a weak innate immune response in ZF. Specifically, the expression of *lysozyme*, *Il1b*, *il6*, *il8*, *il10*, *tnfa*, *ifng*, *hamp1*, *hamp2* and *leap2*, but not *il21*, was lower in Lev-R *V. alginolyticus*-infected ZF than in Lev-S *V. alginolyticus*-infected ZF, which is consistent with the improved survival of *V. alginolyticus*-infected ZF. These findings explain why antibiotic-resistant pathogens are less easily eliminated than antibiotic-sensitive bacteria.

However, factors that induce the innate immune response are not yet fully understood.

Reports indicate that the metabolome contributes to host anti-infection mechanisms (Wang *et al.*, 2016; Sun *et al.*, 2019; Xu *et al.*, 2019), which motivated us to speculate about the role of different metabolomes in coping with antibiotic-resistant pathogens. To explore this, GC-MS-based metabolomics was used to identify reduced maltose as a characteristic feature of the antibiotic-resistant metabolome as well as reduced expression of innate immunity genes in Lev-R *V. alginolyticus*-infected ZF. Other reports also indicate an association between metabolites and expression of innate immunity (Shapiro *et al.*, 2014; Correa-Oliveira *et al.*, 2016; Haas *et al.*, 2016; Xu *et al.*, 2019).

The present study also demonstrates that exogenous maltose increases the expression and activity of lysozyme and antimicrobial peptides. Lysozyme depresses chemotaxis, oxidative metabolism and the generation of superoxide by neutrophils (Sava, 1996), which may explain why maltose elevated expression of lysozyme but reduced expression of other genes. Thus, these results suggest that maltose contributes to the differential expression of innate immune response genes, especially modulating lysozyme expression and activity. This is the first demonstration, to our knowledge, that metabolomic strategy differs in the innate immune response to antibiotic-resistant and antibiotic-sensitive bacteria. Alternatively, injection of ZF with maltose may alter the osmolarity of ZF internal fluids (Mittal *et al.*, 2009), which could alter tissue surface tension and alter the interaction between pathogen and host. This possibility awaits further investigation (Krens *et al.*, 2017).

Reprogramming the metabolome is a powerful approach to improve the host's ability to eliminate bacterial pathogens (Thompson *et al.*, 2017). In the present study, exogenous maltose is used for metabolome reprogramming to restore the ability of ZF to clear antibiotic-resistant *V. alginolyticus*. As expected, higher lysozyme expression and activity were detected in ZF injected with maltose. Accordingly, faster elimination of the antibiotic-resistant bacteria occurred in ZF injected with maltose leading to higher rates of ZF survival. Therefore, maltose plays a crucial role in the elimination of antibiotic-resistant *V. alginolyticus*, and this crucial biomarker, identified in the metabolome of Lev-R *V. alginolyticus*-infected ZF, can restore an effective innate immune response to eliminate antibiotic-resistant pathogens, such as *V. alginolyticus*.

Evidence indicates that lysozyme is an antibacterial effector of the innate immune system in animals that hydrolyse peptidoglycan (Vanderkelen *et al.*, 2011). The therapeutic effectiveness of lysozyme is based on its ability to control the growth of bacteria and to modulate host immunity against infections. However, information

regarding whether the ability of lysozyme to kill different bacteria is related to its level of expression is not available. We supposed that the ability of lysozyme to kill pathogens depends on the degree of bacterial membrane polarization. To test this idea, we measured the membrane potential of two bacterial strains, Lev-R and Lev-S *V. alginolyticus,* and their binding to lysozyme, showing that they are correlated. Lev-R *V. alginolyticus* displayed lower polarization and lower binding than Lev-S *V. alginolyticus*. Besides, binding to Lev-R *V. alginolyticus* was also related to lysozyme concentration, e.g. when the lysozyme concentration was lower than 50 μg ml^{-1}, the difference was distinct. Furthermore, CCCP, an inhibitor of membrane polarization, decreased the binding of lysozyme to Lev-R and Lev-S *V. alginolyticus*. One possible mechanism is that lysozyme's isoelectric point is 11.35, such that lysozyme is positively charged, while Lev-S *V. alginolyticus* has relatively higher membrane polarization and relatively higher negative charge in binding reaction buffer than Lev-R *V. alginolyticus*. This could explain the greater binding affinity of lysozyme to Lev-S *V. alginolyticus*. When a large increase in lysozyme concentration is promoted by exogenous maltose, binding to Lev-R *V. alginolyticus* increases, causing more efficient Lev-R *V. alginolyticus* elimination (Fig. 8). These results support the conclusion that the high membrane polarization is a critical factor for effective lysozyme binding.

Lev-S *V. alginolyticus* induces a stronger innate immune response in ZF, including higher expression of cationic peptides like *hamp1*, *hamp2* and *leap2*, as well as *lyz*. These molecules are positively charged and prone to bind to the negatively charged bacterial surface. This is consistent with our recent finding that bacterial membrane potential plays a critical role in the recruiting and deposition of complement components on the bacterial surface (Cheng *et al.*, 2019). Interestingly, exogenous maltose promotes the expression of lysozyme and the elimination of pathogens. These findings demonstrate that the rate of elimination of antibiotic-resistant bacteria may depend on lysozyme abundance and bacterial membrane polarization. Furthermore, these findings also indicate that metabolic modulation can promote the innate immune response and clearance of antibiotic-resistant bacteria.

The current study does not identify the mechanism by which maltose regulates lysozyme expression. Maltose can be transported into the cell and degraded to glucose, where it enters the glycolysis pathway. Dietary sugars, including starch, dextrin, maltose, glucose and cellulose, could potentially increase lysozyme level and activity in ZF serum (Kong *et al.*, 2019). However, maltose is more potent than glucose in elevating lysozyme expression. This is consistent with our data that maltose is more abundant in Lev-S *V. alginolyticus*-infected than in Lev-R *V. alginolyticus*-infected ZF, with limited glucose production, highlighting the role of maltose in regulating lysozyme expression.

The regulation of lysozyme transcription has been extensively studied in chicken. Upon stimulation with LPS or other pro-inflammatory molecules, the transcription of lysozyme is rapidly activated by transcription factors NF1 and Fli-1, which displace CTCF (Kontaraki *et al.*, 2000; Lefevre *et al.*, 2003; Lefevre *et al.*, 2008). However, the relationship between sugar metabolism and NF1 and Fli-1-dependent regulation of lysozyme expression has not yet been investigated.

The last thing worthy of mention here is the role of antimicrobial peptides in killing antibiotic-resistant bacteria. As shown in Figs 2D and 6C, the expression of *hamp1, hamp2* and lysozyme is similar. *hamp1* and *hamp2* encode hepcidin, an antimicrobial peptide highly conserved in vertebrates (Shike *et al.*, 2004). Hepcidin also has roles in iron homeostasis in macrophages and is induced under stress (Li *et al.*, 2019). Thus, it is worth exploring this role further.

In summary, the present study indicates that a host can mount different metabolic strategies in response to
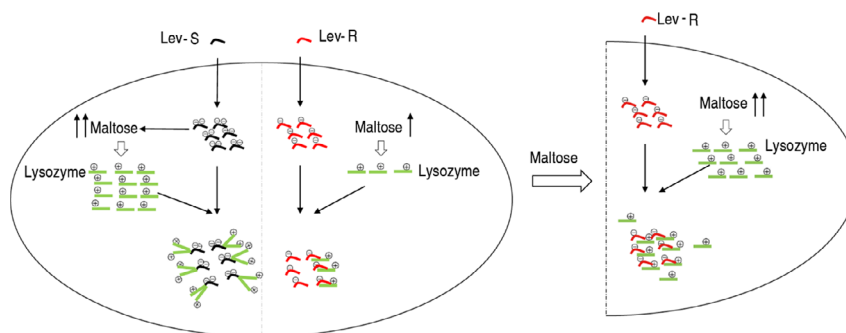
Fig. 8. Proposed model of maltose-induced lysozyme killing of antibiotic-resistant pathogen. Lev-S and Lev-R induce higher and lower lysozyme in ZF respectively. In a neutral buffer, Lev-S has a higher negative electric charge than Lev-R due to its higher membrane potential, while lysozyme has a positive charge. Thus, lysozyme prefers the binding with Lev-S to that with Lev-R. However, maltose increased the amount of lysozyme which enables more binding of lysozyme to Lev-R than before.

infection with antibiotic-sensitive and antibiotic-resistant bacteria and that there is a close relationship between the metabolomic strategy and the innate immune response. Crucial biomarkers associated with the metabolomic strategy lead to differences in the innate immune response, which can be modulated by these biomarkers. These findings highlight the role and potential of metabolomic strategies to promote the innate immune response to antibiotic-resistant pathogens.

Experimental procedures

Ethics statement

This study was conducted following the recommendations in the Guide for the Care and Use of Laboratory Animals of the National Institutes of Health and maintained according to the standard protocols (http://ZFIN. org). All experiments were approved by the Institutional Animal Care and Use Committee of Sun Yat-sen University (Animal welfare Assurance Number: 16).

Bacterial strain and fish

The bacterial strain used in this experiment is *V. alginolyticus* 12G01, a collection of our laboratory. To generate levofloxacin-resistant *V. alginolyticus* (Lev-R), *V. alginolyticus* was subcultured in LB medium with 1/2 minimum inhibitory concentration (MIC) of levofloxacin (0.125 μg) for serial passages, which led to the generation of 16 MIC levofloxacin-resistant *V. alginolyticus.* The *V. alginolyticus* cultured in the same way but in the absence of levofloxacin is named as Lev-S. MIC was determined by antimicrobial susceptibility testing as previously described (Peng *et al.*, 2015). The overnight culture was subcultured in fresh LB medium and grew until the optical density was 0.5 (OD 600 nm) at 30°C. The log-phase cells were diluted and dispensed into 96-well microtitre polystyrene tray with 10^5 cells each well. The tray contained a series of twofold dilutions of antibiotics. After 16 h of incubation, the MIC was defined as the lowest concentration that completely inhibits growth as determined OD at 600 nm. Three biological repeats with two technical replicates were carried out for each sample.

Zebrafish, 45 days post-fertilization (dpf) (0.20 ± 0.03 g in weight and 2.50 ± 0.24 cm in length), were obtained from a zebrafish breeding Corporation, Guangzhou, P.R. China. These animals were free of *Vibrio species* infection through microbiological detection and reared in 25-l open circuit filtered water tanks at room temperature with aeration. They were maintained in our laboratory for another two weeks before experimental manipulation. Zebrafish were fed with regular food Pellet Feed, Shandong Weifang Yeebrand Food Co., LTD, in a maintenance ration so a small and steady growth was expected on a 12/12 h rhythm of light and darkness photoperiod always.

Three-day newborn larvae were obtained as previously described (Winter *et al.*, 2008). Fish were mated in discrete male–female pairs to allow individual clutch use. When sufficient embryos were deposited, they were subjected to an antifungal 'bleaching' procedure: 1% (W/V) chloramine T (Sigma-Aldrich, St Louis, MO, USA) in culture water for 1 min, then two rinces in culture water followed by transfer to a Petri dish containing 0.8 μm sterile-filtered culture water. Throughout the culture period, a Petri dishwater change was undertaken every 24 h to maintain water quality.

Sample preparation for gas chromatography-mass spectrometry (GC-MS) analysis

A total of 660 *D. reiro* were injected with saline ($n = 60$), Lev-S ($n = 300$) or Lev-R ($n = 300$), where the bacterial dose for Lev-S and Lev-R is 9×10^5 CFU per fish. The survival fish were collected and proceed for sample preparation for GC-MS as previously described (Xu *et al.*, 2019). *D. rerio,* 60 dpf, 0.22 ± 0.04g in weight and 2.52 ± 0.31 cm in length, were euthanized in ice slush (5 parts ice/1 part water, 0–4°C) for at least 10 min following cessation of gill movement and left in the ice water for a total of 20 min after cessation of all movement to ensure death by hypoxia following the guidelines of NIH (Reed and Jennings, 2011). *D. rerio* were rinsed with distilled water and then wiped thoroughly with sterilized gauze. Each fish was cut into five pieces on ice so the metabolites of the body fluids will diffuse out and then weighted. The appropriate volume of saline (100 μl 100 mg^{-1}) was added according to the weight. After centrifugation at 3000 g at 4°C, 100 μl fluid was aliquoted for the following metabolomic analysis. Metabolites were extracted with 0.2 ml of cold methanol, containing 10 μl of 0.1 mg ml^{-1} ribitol (Sigma-Aldrich) as an analytical internal standard. After centrifugation at 12 000 g for 10 min, the supernatant was concentrated in a rotary vacuum centrifuge device, LABCONCO. The dried polar extracts were used for GC-MS analysis.

Gas chromatography–mass spectrometry (GC-MS) analysis

The GC-MS analysis was carried out with a variation on the two-stage techniques as described previously (Su *et al.*, 2018). In brief, samples were derivatized in 40 μl of 20 mg ml^{-1} methoxyamine hydrochloride (Sigma-Aldrich) in pyridine to protect carbonyl moieties through methoximation for 90 min at 37°C, followed by adding 80 μl of *N*-methyl-*N*-trimethylsilyl trifluoroacetamide (MSTFA) for derivatization of acidic protons (Sigma-Aldrich) at 37°C for

another 30 min. The derivatized sample of 1 μl was injected into a 30 m × 250 μm i.d. × 0.25 μm DBS-MS column using splitless injection, and analysis was carried out in Agilent 7890A GC equipped with an Agilent 5975C VL MSD detector, Agilent Technologies. The initial temperature of the GC oven was held at 85°C for 5 min followed by an increase to 270°C at a rate of 15°C min^{-1} then held for 5 min. Helium was used as the carrier gas and flow was kept constantly at 1 ml min^{-1}. The MS was operated in a range of 50–600 m/z. For each sample, two technical replicates were prepared to confirm the reproducibility of the reported procedures.

Metabolites were identified following the guidelines of the metabolomics standards initiative (Sumner *et al.*, 2007). In conclusion, the deconvolution and calibration of the acquired mass spectra were performed with AMDIS (Agilent Open LAB CDS ChemiStation C.01.01). To avoid false positives, peaks with a signal-to-noise ratio (S/N) lower than 30 were excluded (Pezzatti *et al.*, 2019). Additionally, the artefact peaks were removed through comparison with the blank samples. Metabolites were identified by retrieving their mass spectra in the NIST 2011 (National Institute of Standards and Technology, Gaithersburg, MD, USA) library and GMD 2011 (Golm Metabolome Database, Potsdam, Germany) according to the following criteria: match value ≥ 750, reverse match value ≥ 800 and a probability ≥ 60% (Zhu *et al.*, 2016). The relative peak area value of the ribitol was taken as the internal standard to calculate the metabolite abundance.

Exogenous addition of maltose and bacterial challenge

D. rerio were randomly divided into control and test groups and acclimatized for 14 days at 28°C after purchase from the fish corporation. Thirty individuals were included in each group. *D. rerio* were anesthetized by immersing in 0.02% tricaine methanesulfonate solution, which was subsequently injected with 225 μg maltose, a dose that was estimated from the average concentration of maltose after Lev-S infection (225 μg per fish), into individual *D. rerio* as test group or the same volume of sterile saline as control group. Both groups were injected once daily for 3 days. After the last shot, *D. rerio* were challenged by intramuscular injection of 1.0 × 10^6 CFU of Lev-S/fish or 3.0 × 10^6 CFU of Lev-R/fish. These zebrafish were observed for symptoms twice daily for 15 days for accumulative death.

Sample preparation of zebrafish in the presence or absence of exogenous maltose

Bacteria were grown in 100 ml LB medium at 30°C overnight and then diluted 1:100 into fresh LB medium until its absorbance value of OD600 equal to 0.2. Then, the cells were washed with a saline buffer three times and were resuspended in saline buffer. *D. rerio* were divided into two groups treated with and without maltose. The group with maltose was injected with 225 μg maltose with a microlitre syringe (scale from 0.00 to 0.05 ml), Shanghai Gaoge Industrial and Trading Co.LTD, China, as test group and the group without maltose were injected with the same volume of sterile saline as a control group for three days. Samples were collected for lysozyme activity assay by commercial kit and maltose quantification by UPLC-MS. Meanwhile, each of the other fish from the two groups was challenged with 2 × 10^5 CFU of Lev-R by intramuscular injection. For qPCR detection of bacterial counts, *D. rerio* at 0, 6, 24, 48, 72 h post-injection were euthanized in ice slush (5 parts ice/1 part water, 0–4°C) for at least 10 min following cessation of gill movement, and left in the ice water for a total of 20 min after cessation of all movement to ensure death by hypoxia following the guidelines of NIH (Reed and Jennings, 20112011). Total DNA was extracted from samples with DNeasy Blood & Tissue Kit (Qiagen, Hilden, Germany), according to the manufacturer's instructions. The purified DNA was stored at − 20°C for qPCR amplification. The experiment was performed in six biological replicates. For qRT-PCR detection of innate immune genes, *D. rerio* at 6 h post-injection was anesthetized in 0.02% tricaine methanesulfonate solution. Spleens and head kidneys were removed ascetically and were stored at −80°C until RNA extraction. Spleens or head kidneys from three *D. rerio* were pooled as one sample for RNA isolation. To perform qRT-PCR in *D. rerio* newborn larvae, larvae of 3 days dpf were collected and immersed in 1 × 10^5 V. *alginolyticus* in Hank's buffer for three days. After infection, larvae were immediately collected and three larvae were pooled as one sample for RNA isolation.

Total RNA was isolated with Trizol (Invitrogen, Carlsbad, CA, USA) and RNA was then quantified by Nano-Drop, Thermo Scientific. Reverse transcription-PCR was carried out on a Prime-Script^{TM} RT reagent Kit with gDNA eraser (Takara, Kusatsu, Shiga, Japan) with 1 μg of total RNA according to manufacturer's instructions. The experiment was performed in six biological replicates.

Bacterial membrane polarization

Membrane polarization was carried out as described previously (Su *et al.*, 2018). DiOC2(3), a fluorescent membrane potential indicator dye, was applied to investigate the bacterial membrane potential (membrane polarization). Bacteria were obtained from log-phase cultures and diluted to approximately 1 × 10^6 cells per ml in filtered saline. These bacteria were treated with or without 1 mM CCCP for 30 min. Then, a volume of 10 μl of

3 mM DiOC2(3) was added and then incubated at room temperature for 30 min. Stained bacteria were assayed with a flow cytometer equipped with a laser emitting at 488 nm. Fluorescence was measured on the green and red channels ('GC' and 'RC'), and filters were used to detect fluorescein and Texas Red dye respectively. Because the relative amount of red and green fluorescence intensity varied with cell size and aggregation, the ratio of red to green fluorescence intensity was used as a size-independent indicator of membrane potential.

Quantitative analysis of lysozyme captured by Lev-S and Lev-R

Bacteria were grown in 100 ml LB medium at 30°C overnight. Bacteria were washed three times with saline buffer and were resuspended in saline to OD 600 at 1.0. A doubling dilution series ranging from 6.25 to 400 μg ml^{-1} of lysozyme, Sangon Biotech, Shanghai, China, were used for quantitative analysis of lysozyme captured by Lev-R or Lev-S. The resuspended cells were mixed with 200 μl lysozyme at 4°C for 16 h. For the experiment with carbonyl cyanide 3-chlorophenylhydrazone (CCCP), bacteria were pretreated with different CCCP for 30 min before adding lysozyme. After incubation, the mixture was washed with cold saline, followed by washing with 200 μl 0.1 M Gly-HCl buffer (pH 2.4). Finally, the mixture was centrifuged at 7000 g for 15 min at 4°C, the supernatant was collected and neutralized with 1 M Tris–HCl (pH 8.8), and stored at −20°C until lysozyme activity assay.

Lysozyme assay

Lysozyme Assay Kit was purchased from the Nanjing Jiancheng Bioengineering Institute, China. The activity of lysozyme in zebrafish body fluid and captured by Lev-S and Lev-R was determined according to the method based on the lysis of the lysozyme-sensitive Gram-positive bacteria *Micrococcus lysodeikticus.* Shortly, 2 ml of *M. lysodeikticus* (g-type) lysozyme (Sigma-Aldrich) at a concentration of 0.2 mg ml^{-1} (w/v) in 50 mM phosphate buffer (pH 6.2) and 100 μl body fluid or reaction mixture was added. The reduction in absorbance at 530 nm was measured after 15 min water bath at 37°C. Results were expressed in units of lysozyme ml^{-1}. One unit was defined as the amount of sample causing a decrease in absorbance of 0.001 units per min.

Lysozyme bactericidal assay/lysozyme plus serum bactericidal assay

A single bacterial colony was grown in 50 ml LB broth in 250-ml flasks for 24 h at 30°C. After centrifugation at 8000 rpm for 5 min, samples were washed twice with 30 ml sterile saline and resuspended in M9 minimal media supplemented with 10 mM acetate, 1 mM MgSO$_4$ and 100 mM CaCl$_2$ to 0.2 at OD600. Lysozyme (g-type) or lysozyme plus serum was added and incubated at 30°C for 1 h. After incubation, 100 ml aliquot samples were periodically removed, serially diluted and plated (10 ml aliquots) onto LB agar plates. The plates were cultured at 30°C for 8 h. Only those dilutions yielding 20–200 colonies were enumerated to calculate colony-forming units (CFUs). Per cent survival was determined by dividing the CFU obtained from a treated sample by the CFU obtained from control.

Cell culture and promoter activity assay

Danio rerio cell line, ZF4, was purchased from the Institute of hydrobiology, China, and was maintained in DMEM: F12 medium, GIBICO, Life Technologies, supplemented with 10% foetal bovine serum. Cells were grown in a humidified incubator at 5% CO$_2$ and 28°C.

To perform promoter activity assay, the 1500 bp upstream of the exon 1 (primers were shown in Table S3) were amplified by PCR and cloned into a promoterless vector, pGL3.0-Basic, upstream of the firefly luciferase gene. The insert was confirmed by sequencing. ZF4 cells were harvested using 0.25% (W/V) trypsin solution and seed into 24-well plates at a density of 2.5×10^5 cells per well. The plasmid was transfected into the cell with polyethyleneimine. To minimize non-relevant influences, an additional vector (pRL-TK) containing the Renilla luciferase gene was co-transfected. After an incubation time of 24 h, the cells were co-cultured with 1×10^6 Lev-s or Lev-R for 3 h. Then, the cells were lysed and incubated with luciferin according to the manufacturer's instructions. The luciferase activity of the promoter-firefly luciferase constructs was then normalized to the Renilla luciferase activity derived from the pRL-TK vector and expressed as relative fold.

Statistical analysis

Data shown are the means $\pm$ SEM. The Gaussian distribution of data was analysed by D'Agostino-Pearson omnibus normality test (Prism 7.0, GraphPad Software, San Diego, CA, USA) and Kolmogorov–Smirnov test (Prism 7.0). The variance of data was analysed by the homogeneity of variance test (SPSS 22.0, IBM Corp, Armonk, NY, USA) or Brown–Forsythe test (Prism 7.0).

As none of the dependent variables comply with the ANOVA assumptions of normality, therefore, data for one-factorial design were analysed by Kruskal–Wallis followed by Dunn's multiple comparison *post hoc* test. (Prism 7.0). Data for 2-factorial designs were analysed by Aligned Rank Transform procedure with ANOVA (ART-ANOVA), and ART-ANOVA is a non-parametric factorial analysis

technique recently introduced by Wobbrock *et al.* (2011), which enables the use of ANOVA test after alignment and ranking and maintains the integrity of interaction effects of factors. Statistical details of all experiments can be found in the figure legends, and significance is described in the figure legends as $*P < 0.05$, $**P < 0.01$.

The multivariate analysis

The multivariate analysis was performed using principal component analysis (PCA) and orthogonal partial least squares discriminant analysis (OPLS-DA) with SIMCA 12.0 software (Umetrics, Umeå, Sweden). PCA was used to describe the sample variations between groups (Saline, Lev-S, and Lev-R) in the scoring matrix. OPLS-DA was used to assign samples according to the classes, variability in the S-Plot. The potential biomarkers were selected when p(corr) > 0.5 combined with $P \geq 0.05$.

Conflicts of interest

None declared.

Author contributions

BP conceptualized and designed the project. MJ, LFY, ZGC and SSL performed experiments. MJ, LFY and SSL performed data analysis. BP, MJ and ZGC interpreted the data. BP wrote the manuscript. All the authors reviewed the manuscript.

References

Abdallah, F.B., Chaieb, K., Kallel, H., and Bakhrouf, A. (2009) RT-PCR assays for in vivo expression of *Vibrio alginolyticus* virulence genes in cultured gilthead *Dicentrarchus labrax* and *Sparus aurata*. *Ann Microbiol* **59:** 63–67.

Andersson, D.I. (2003) Persistence of antibiotic resistant bacteria. *Curr Opin Microbiol* **6:** 452–456.

Andersson, D.I., and Hughes, D. (2010) Antibiotic resistance and its cost: is it possible to reverse resistance? *Nat Rev Microbiol* **8:** 260–271.

Araldi, E., Fernandez-Fuertes, M., Canfran-Duque, A., Tang, W., Cline, G.W., Madrigal-Matute, J., *et al.* (2017) Lanosterol modulates TLR4-mediated innate immune responses in macrophages. *Cell Rep* **19:** 2743–2755.

Avci, F. Y., Li, X., Tsuji, M., and Kasper, D.L. (2013) Carbohydrates and T cells: a sweet twosome. *Semin Immunol* **25:** 146–151.

Bergers, J.J., Vingerhoeds, M.H., van Bloois, L., Herron, J.N., Janssen, L.H., Fischer, M.J., *et al.* (1993) The role of protein charge in protein-lipid interactions. pH-dependent changes of the electrophoretic mobility of liposomes through adsorption of water-soluble, globular proteins. *Biochemistry-Us* **32:** 4641–4649.

Cameron, A.M., Lawless, S.J., and Pearce, E.J. (2016) Metabolism and acetylation in innate immune cell function and fate. *Semin Immunol* **28:** 408–416.

Cheng, S.C., Quintin, J., Cramer, R.A., Shepardson, K.M., Saeed, S., Kumar, V., *et al.* (2014) mTOR- and HIF-1alpha-mediated aerobic glycolysis as metabolic basis for trained immunity. *Science* **345:** 1250684.

Cheng, Z.X., Guo, C., Chen, Z.G., Yang, T.C., Zhang, J.Y., Wang, J., *et al.* (2019) Glycine, serine and threonine metabolism confounds efficacy of complement-mediated killing. *Nat Commun* **10:** 3325.

Correa-Oliveira, R., Fachi, J.L., Vieira, A., Sato, F.T., and Vinolo, M.A. (2016) Regulation of immune cell function by short-chain fatty acids. *Clin Transl Immunology* **5:** e73.

Crocker, P.R., and Feizi, T. (1996) Carbohydrate recognition systems: functional triads in cell-cell interactions. *Curr Opin Struct Biol* **6:** 679–691.

Danese, P.N., and Silhavy, T.J. (1998) CpxP, a stress-combative member of the Cpx regulon. *J Bacteriol* **180:** 831–839.

Faikoh, E.N., Hong, Y.H., and Hu, S.Y. (2014) Liposome-encapsulated cinnamaldehyde enhances zebrafish (*Danio rerio*) immunity and survival when challenged with Vibrio vulnificus and *Streptococcus agalactiae*. *Fish Shellfish Immunol* **38:** 15–24.

Gammoh, N.Z., and Rink, L. (2017) Zinc in Infection and Inflammation. *Nutrients* **9:624.**

Gandon, S., and Vale, P.F. (2014) The evolution of resistance against good and bad infections. *J Evol Biol* **27:** 303–12.

Gong, Q., Yang, D., Jiang, M., Zheng, J., and Peng, B. (2020) l-aspartic acid promotes fish survival against Vibrio alginolyticus infection through nitric oxide-induced phagocytosis. *Fish Shellfish Immunol* **97:** 359–366.

Gorbenko, G.P., Ioffe, V.M., and Kinnunen, P.K. (2007) Binding of lysozyme to phospholipid bilayers: evidence for protein aggregation upon membrane association. *Biophys J* **93:** 140–153.

Haas, R., Cucchi, D., Smith, J., Pucino, V., Macdougall, C.E., and Mauro, C. (2016) Intermediates of metabolism: from bystanders to signalling molecules. *Trends Biochem Sci* **41:** 460–471.

Kong, Y., Ding, Z., Zhang, Y., Zhou, P., Wu, C., Zhu, M., *et al.* (2019) Types of carbohydrate in feed affect the growth performance, antioxidant capacity, immunity, and activity of digestive and carbohydrate metabolism enzymes in juvenile Macrobrachium nipponense. *Aquaculture* **512:** 734282.

Kontaraki, J., Chen, H.H., Riggs, A., and Bonifer, C. (2000) Chromatin fine structure profiles for a developmentally regulated gene: reorganization of the lysozyme locus before trans-activator binding and gene expression. *Genes Dev* **14:** 2106–2122.

Kovarik, P., Castiglia, V., Ivin, M., and Ebner, F. (2016) Type i interferons in bacterial infections: a balancing act. *Front Immunol* **7:** 652.

Kraemer, S.A., Ramachandran, A., and Perron, G.G. (2019) Antibiotic pollution in the environment: from microbial ecology to public policy. *Microorganisms* **7:** 180.

Krens, S., Veldhuis, J.H., Barone, V., Capek, D., Maitre, J.L., Brodland, G.W., *et al.* (2017) Interstitial fluid

osmolarity modulates the action of differential tissue surface tension in progenitor cell segregation during gastrulation. *Development* **144:** 1798–1806.

Lee, H.H., and Collins, J.J. (2011) Microbial environments confound antibiotic efficacy. *Nat Chem Biol* **8:** 6–9.

Lefevre, P., Melnik, S., Wilson, N., Riggs, A.D., and Bonifer, C. (2003) Developmentally regulated recruitment of transcription factors and chromatin modification activities to chicken lysozyme cis-regulatory elements in vivo. *Mol Cell Biol* **23:** 4386–4400.

Lefevre, P., Witham, J., Lacroix, C.E., Cockerill, P.N., and Bonifer, C. (2008) The LPS-induced transcriptional upregulation of the chicken lysozyme locus involves CTCF eviction and noncoding RNA transcription. *Mol Cell* **32:** 129–139.

Li, Z., Wang, Y., Li, X., Lin, Z., Lin, Y., Srinivasan, R., *et al.* (2019) The characteristics of antibiotic resistance and phenotypes in 29 outer-membrane protein mutant strains in *Aeromonas hydrophila*. *Environ Microbiol* **21:** 4614–4628.

Mittal, R., Sharma, S., Chhibber, S., and Harjai, K. (2009) Effect of osmolarity on virulence of uropathogenic *Pseudomonas aeruginosa*. *Am J Biomed Sci* **1:12–26.**

Newton, A., Kendall, M., Vugia, D.J., Henao, O.L., and Mahon, B.E. (2012) Increasing rates of vibriosis in the United States, 1996–2010: review of surveillance data from 2 systems. *Clin Infect Dis* **54(Suppl.** 5): S391–S395.

Peng, B., Su, Y.B., Li, H., Han, Y., Guo, C., Tian, Y.M., *et al.* (2015) Exogenous alanine and/or glucose plus kanamycin kills antibiotic-resistant bacteria. *Cell Metab* **21:** 249–262.

Peng, B., Li, H., and Peng, X.X. (2015) Functional metabolomics: from biomarker discovery to metabolome reprogramming. *Protein Cell* **6:** 628–637.

Pezzatti, J., Gonzalez-Ruiz, V., Codesido, S., Gagnebin, Y., Joshi, A., Guillarme, D., *et al.* (2019) A scoring approach for multi-platform acquisition in metabolomics. *J Chromatogr A* **1592:** 47–54.

Raivio, T.L., Leblanc, S.K., and Price, N.L. (2013) The *Escherichia coli* Cpx envelope stress response regulates genes of diverse function that impact antibiotic resistance and membrane integrity. *J Bacteriol* **195:** 2755–2767.

Reed, B., and Jennings, M. (2011) *Guidance on the Housing and Care of Zebrafish Danio rerio*. ID - 20133283946. Horsham: Royal Society for the Prevention of Cruelty to Animals (RSPCA); 2011.

Roux, D., Danilchanka, O., Guillard, T., Cattoir, V., Aschard, H., Fu, Y., *et al.* (2015) Fitness cost of antibiotic susceptibility during bacterial infection. *Sci Transl Med* **7:** 114r–297r.

Sava, G. (1996) Pharmacological aspects and therapeutic applications of lysozymes. *EXS* **75:** 433–449.

Shapiro, H., Thaiss, C.A., Levy, M., and Elinav, E. (2014) The cross talk between microbiota and the immune system: metabolites take center stage. *Curr Opin Immunol* **30:** 54–62.

Shike, H., Shimizu, C., Lauth, X., and Burns, J.C. (2004) Organization and expression analysis of the zebrafish hepcidin gene, an antimicrobial peptide gene conserved among vertebrates. *Dev Comp Immunol* **28:** 747–754.

Sperling, L., Alter, T., and Huehn, S. (2015) Prevalence and antimicrobial resistance of *Vibrio* spp. In retail and farm shrimps in ecuador. *J Food Prot* **78:** 2089–2092.

Su, Y.B., Peng, B., Han, Y., Li, H., and Peng, X.X. (2015) Fructose restores susceptibility of multidrug-resistant Edwardsiella tarda to kanamycin. *J Proteome Res* **14:** 1612–1620.

Su, Y.B., Peng, B., Li, H., Cheng, Z.X., Zhang, T.T., Zhu, J.X., *et al.* (2018) Pyruvate cycle increases aminoglycoside efficacy and provides respiratory energy in bacteria. *Proc Natl Acad Sci USA* **115:** E1578–E1587.

Sumner, L.W., Amberg, A., Barrett, D., Beale, M.H., Beger, R., Daykin, C.A., *et al.* (2007) Proposed minimum reporting standards for chemical analysis Chemical Analysis Working Group (CAWG) Metabolomics Standards Initiative (MSI). *Metabolomics* **3:** 211–221.

Sun, L., Yao, Z., Guo, Z., Zhang, L., Wang, Y., Mao, R., *et al.* (2019) Comprehensive analysis of the lysine acetylome in *Aeromonas hydrophila* reveals cross-talk between lysine acetylation and succinylation in LuxS. *Emerg Microbes Infect* **8:** 1229–1239.

Thomas, R., and Yang, X. (2016) NK-DC Crosstalk in immunity to microbial infection. *J Immunol Res* **2016:** 1–7.

Thompson, A.A., Dickinson, R.S., Murphy, F., Thomson, J.P., Marriott, H.M., Tavares, A., *et al.* (2017) Hypoxia determines survival outcomes of bacterial infection through HIF-1alpha dependent re-programming of leukocyte metabolism. *Sci Immunol* **2:eaal2861.**

Vanderkelen, L., Van Herreweghe, J.M., Vanoirbeek, K.G., Baggerman, G., Myrnes, B., Declerck, P.J., *et al.* (2011) Identification of a bacterial inhibitor against g-type lysozyme. *Cell Mol Life Sci* **68:** 1053–1064.

Wang, Z., Li, M.Y., Peng, B., Cheng, Z.X., Li, H., and Peng, X.X. (2016) GC-MS-based metabolome and metabolite regulation in serum-resistant *Streptococcus agalactiae*. *J Proteome Res* **15:** 2246–2253.

Wang, Y.D., Wang, Y.H., Hui, C.F., and Chen, J.Y. (2016) Transcriptome analysis of the effect of *Vibrio alginolyticus* infection on the innate immunity-related TLR5-mediated induction of cytokines in *Epinephelus lanceolatus*. *Fish Shellfish Immunol* **52:** 31–43.

Winter, M.J., Redfern, W.S., Hayfield, A.J., Owen, S.F., Valentin, J.P., and Hutchinson, T.H. (2008) Validation of a larval zebrafish locomotor assay for assessing the seizure liability of early-stage development drugs. *J Pharmacol Toxicol Methods* **57:** 176–187.

Wobbrock, J.O., Findlater, L., Gergle, D., and Higgins, J.J. (2011) The aligned rank transform for nonparametric factorial analyses using only anova procedures. In *Proceedings of the SIGCHI Conference on Human Factors in Computing Systems*. Vancouver, BC: Association for Computing Machinery, pp. 143–146.

Wyrsch, E.R., Roy, C.P., Chapman, T.A., Charles, I.G., Hammond, J.M., and Djordjevic, S.P. (2016) Genomic microbial epidemiology is needed to comprehend the global problem of antibiotic resistance and to improve pathogen diagnosis. *Front Microbiol* **7:** 843.

Xie, Z.Y., Hu, C.Q., Chen, C., Zhang, L.P., and Ren, C.H. (2005) Investigation of seven Vibrio virulence genes among *Vibrio alginolyticus* and *Vibrio parahaemolyticus*

strains from the coastal mariculture systems in Guang-dong, China. *Lett Appl Microbiol* **41:** 202–207.

Xu, D., Wang, J., Guo, C., Peng, X.X., and Li, H. (2019) Elevated biosynthesis of palmitic acid is required for zeb-rafish against *Edwardsiella tarda* infection. *Fish Shellfish Immunol* **92:** 508–518.

Zhang, Y.L., Peng, B., Li, H., Yan, F., Wu, H.K., Zhao, X.L., *et al.* (2017) C-terminal domain of hemocyanin, a major antimicrobial protein from litopenaeus vannamei: structural homology with immunoglobulins and molecular diversity. *Front Immunol* **8:** 611.

Zhang, S., Wang, J., Jiang, M., Xu, D., Peng, B., Peng, X.X., *et al.* (2019) Reduced redox-dependent mechanism and glucose-mediated reversal in gentamicin-resistant *Vibrio alginolyticus*. *Environ Microbiol* **21:** 4724–4739.

Zhu, W., Zhang, H., Li, X., Meng, Q., Shu, R., Wang, M., *et al.* (2016) Cold adaptation mechanisms in the ghost moth *Hepialus xiaojinensis*: metabolic regulation and ther-mal compensation. *J Insect Physiol* **85:** 76–85.

Supporting information

Additional supporting information may be found online in the Supporting Information section at the end of the article.

Fig. S1. Well-plate map for determination of MIC for Lev-S and Lev-R in 96-well plate.

Fig. S2. Determination of LD50 of Lev-S and Lev-R.

Fig. S3. (A) Ct values of gyrB in different CFU of Lev-S and Lev-R (B) Standard curve for detection of *gyrB* gene in ZF.

Fig. S4. Lev-S and Lev-R loads in ZF.

Fig. S5. Cell viability after being challenged with Lev-S (A) or Lev-R (B). (C) Luciferase activity was monitored at differ-ent time points as indicated.

Fig. S6. Lev-R loads in ZF with or without maltose.

Fig. S7. (A) Growth curve of Lev-S and Lev-R. OD600 was read at each time point. (B) The area under the growth curve of Lev-S and Lev-R in (A). (C) Effect of exogenous maltose on Lev-S and Lev-R growth. (D) qRT-PCR for viru-lent genes of Lev-S and Lev-R grew in rich medium supple-mented with additional maltose. (E) qRT-PCR for virulent genes of Lev-S and Lev-R grew in minimal medium supple-mented with additional maltose.

Fig. S8. Heat map showing the relative abundance of metabolites (Wilcoxon *P* < 0.01) in Lev-R, Lev-S and saline control.

Table S1. Statistics of scaffold assembled from wildtype sample.

Table S2. Annotation for mutations idenitfied from mutant against to wildtype.

Table S3. Primers used for PCR and RT-qPCR analysis.